



Missouri University of Science and Technology
Scholars' Mine

Electrical and Computer Engineering Faculty
Research & Creative Works

Electrical and Computer Engineering

01 Jan 2004

Manipulation of Microenvironment with a Built-in Electrochemical Actuator in Proximity of a Dissolved Oxygen Microsensor

Chang-Soo Kim

Missouri University of Science and Technology, ckim@mst.edu

J. O. Fiering

C. W. Scarantino

H. Troy Nagle

et. al. For a complete list of authors, see https://scholarsmine.mst.edu/ele_comeng_facwork/1708

Follow this and additional works at: https://scholarsmine.mst.edu/ele_comeng_facwork



Part of the [Biology Commons](#), and the [Electrical and Computer Engineering Commons](#)

Recommended Citation

C. Kim et al., "Manipulation of Microenvironment with a Built-in Electrochemical Actuator in Proximity of a Dissolved Oxygen Microsensor," *IEEE Sensors Journal*, Institute of Electrical and Electronics Engineers (IEEE), Jan 2004.

The definitive version is available at <https://doi.org/10.1109/JSEN.2004.832857>

This Article - Journal is brought to you for free and open access by Scholars' Mine. It has been accepted for inclusion in Electrical and Computer Engineering Faculty Research & Creative Works by an authorized administrator of Scholars' Mine. This work is protected by U. S. Copyright Law. Unauthorized use including reproduction for redistribution requires the permission of the copyright holder. For more information, please contact scholarsmine@mst.edu.

Manipulation of Microenvironment With a Built-In Electrochemical Actuator in Proximity of a Dissolved Oxygen Microsensor

Chang-Soo Kim, *Member, IEEE*, Chae-Hyang Lee, Jason O. Fiering, Stefan Ufer, *Associate Member, IEEE*, Charles W. Scarantino, and H. Troy Nagle, *Fellow, IEEE*

Abstract—Biochemical sensors for continuous monitoring require dependable periodic self diagnosis with acceptable simplicity to check its functionality during operation. An *in-situ* self-diagnostic technique for a dissolved oxygen microsensor is proposed in an effort to devise an intelligent microsensor system with an integrated electrochemical actuation electrode. With a built-in platinum microelectrode that surrounds the microsensor, two kinds of microenvironments, called the oxygen-saturated or oxygen-depleted phases, can be created by water electrolysis, depending on the polarity. The functionality of the microsensor can be checked during these microenvironment phases. The polarographic oxygen microsensor is fabricated on a flexible polyimide substrate (Kapton) and the feasibility of the proposed concept is demonstrated in a physiological solution. The sensor responds properly during the oxygen-generating and oxygen-depleting phases. The use of these microenvironments for *in-situ* self-calibration is discussed to achieve functional integration, as well as structural integration, of the microsensor system.

Index Terms—Electrolysis, intelligent microsensor, polyimide, self calibration, self diagnosis.

I. INTRODUCTION

AN INTELLIGENT microsensor system requires not only structural integration, but also functional integration. In a biochemical microsensor system, special functionalities can be provided by the use of electrochemical “actuators” integrated with the sensor. Several electrochemical microactuators utilizing redox reactions of chemical species have been reported in combination with microsensors. A microscale pH titration system was first implemented by integrating a titration microelectrode with ion-sensitive field-effect transistor (pH-ISFET)

Manuscript received July 24, 2001; revised February 20, 2004. This work was supported in part by the NASA Office of Biological and Physical Research under Grant NAG9-1423 and in part by Sidel Technologies, Inc., Research Triangle Park, NC. The associate editor coordinating the review of this paper and approving it for publication was Prof. Elias Towe.

C.-S. Kim and C.-H. Lee are with the Department of Electrical and Computer Engineering and Biological Sciences, University of Missouri-Rolla, Rolla, MO 65409 USA (e-mail: ckim@umr.edu; leecha@umr.edu).

J. O. Fiering is with Draper Laboratory, Cambridge, MA 02139 USA (e-mail: jfiering@draper.com).

S. Ufer and H. T. Nagle are with Biomedical MicroSensors Laboratory, Department of Electrical and Computer Engineering, North Carolina State University, Raleigh, NC 27695-7911 USA (e-mail: t.nagle@ncsu.edu; stufer@eos.ncsu.edu).

C. W. Scarantino is with Sidel Technologies, Inc., Morrisville, NC 27560 USA (e-mail: cw.scarantino@rexhealth.com).

Digital Object Identifier 10.1109/JSEN.2004.832857

[1]. Based on this concept, a long-term measurement of dissolved carbon dioxide was performed without the need for regular recalibration [2]. A similar structure has been used to demonstrate a potentiometric dissolved oxygen sensor based on pH sensing [3], which was later adopted in simultaneous measurement of cellular respiration and acidification with a single sensor [4]. With built-in iridium oxide actuators on top of the gate region of field-effect transistor (FET), novel potentiometric determinations of dissolved oxygen [5] and hydrogen peroxide [6] were accomplished. Microfluidic systems including electrochemical actuators and sensors were reported to detect flow direction and to estimate flow velocity [7], [8]. Novel biosensors with built-in electrochemical actuation systems include a pH-static enzyme sensor to suppress the dependency of sensor response on sample solution pH [9] and a high-sensitivity potentiometric glucose sensor with the aid of an amperometric actuation system [10].

An ideal biosensor for long-term continuous monitoring should meet the following requirements: simple structure, immunity to motion artifacts, sufficient sensitivity for reliable measurements, robustness and stability over long periods of time, minimum inflammatory reaction with surrounding tissues during chronic implantation, and dependable diagnosis and/or calibration methods to check its functionality and accuracy. Numerous types of sensors for dissolved oxygen monitoring have been developed over the past decades (for a review, see [11] and [12]), and only limited successes have been achieved in spite of intensive efforts to meet these requirements. Apart from such long-term stability or biocompatibility, it should be emphasized that development of a novel *in-situ* diagnosis technique without any externally coupled apparatus is one obstacle to the realization of an unattended intelligent microsensor system. Consequently, we present a novel self-diagnosis concept for a dissolved oxygen microsensor by using an integrated electrochemical microactuator toward built-in intelligence of the microsensor system.

II. IN-SITU SELF-DIAGNOSIS CONCEPT WITH ELECTROCHEMICAL MICROACTUATOR

The principle of the novel diagnosis method proposed herein is based on water electrolysis at noble metal electrodes as shown in Fig. 1. Oxygen or hydrogen can be generated by the electrolysis of water in a controlled manner by applying voltage or

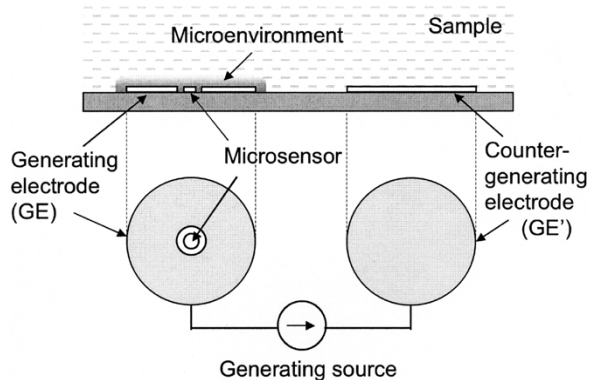
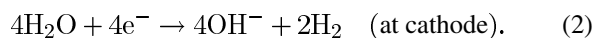
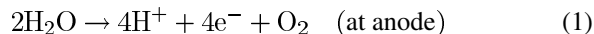


Fig. 1. Concept for a novel oxygen sensor with *in-situ* self-diagnosis capability. The microenvironment is generated by a GE which surrounds the microsensor. Oxygen-saturated or oxygen-depleted phases can be established by water electrolysis depending on the polarity.

current through a generating electrode (GE) and counter-generating electrode (GE') [13]. Reactions occurring at the anode and cathode are as follows:



Accumulation of these dissolved gas molecules at the GE, in turn, rapidly establishes a microenvironment of oxygen saturation or hydrogen saturation. The accumulation and saturation of hydrogen molecules takes place after the depletion of oxygen. An oxygen microsensor in close proximity to the surrounded GE can be confined in a controlled microenvironment. A two-point self-diagnostic procedure for the oxygen sensor can then be performed, with the high-point diagnosis being established in an oxygen-saturated phase, and the low-point diagnosis in an oxygen-depleted phase, respectively. These transient perturbations of the microenvironment are expected to equilibrate rapidly with the surrounding solution medium.

III. METHODS

A. Device Design

We designed and fabricated polarographic micro-oxygen sensors on flexible polyimide substrates (Kapton). The basic electrochemical three electrode cell configuration was adopted to avoid the ohmic voltage drop through the electrolyte between the anode and cathode. All electrodes were designed to be geometrically symmetric to assure diffusional mass transport of electrochemical species in all radial directions. The noise at an electrode–electrolyte interface can be modeled by two sources [14]— $1/f$ noise and white noise. The $1/f$ noise is inversely proportional to the electrode area. A lower form factor for the electrode (the circumference to surface area ratio) results in a lower white noise level, which implies that the noise generated by a circular-type electrode is lower than any other type of electrodes. Therefore we used a circular working electrode (WE). The conventional Clark oxygen sensor contains a reference electrode (RE) and a WE located in the same compartment filled with an internal electrolyte gel which is encapsulated by a hydrophobic, electrically nonconducting membrane. To circumvent the technical difficulties of fabricating the reliable

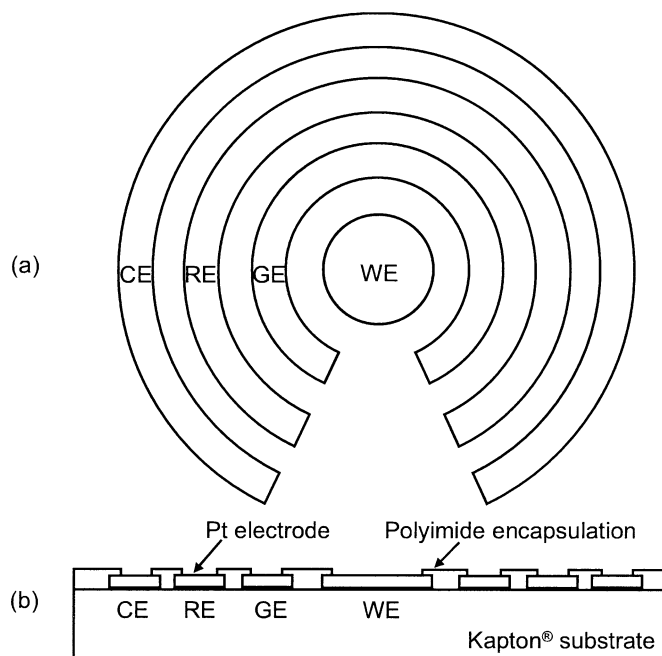


Fig. 2. Concentric three-electrode oxygen sensor with total diameter of $200 \mu\text{m}$. (a) Layout of exposed electrodes (not to scale). (b) Cross-sectional view after fabrication on a flexible Kapton substrate (substrate cleaning, Au/Cr deposition, Pt/Ti deposition, Pt/Ti lift off, Au/Cr etching, and polyimide patterning).

double-layered membrane (electrolyte gel/hydrophobic membrane) [15], [16], we did not use any membrane in this study.

Fig. 2 shows the layout and cross section of the concentric-type electrode configuration. The middle electrode serves as the WE at which dissolved oxygen molecules are cathodically reduced. The GE is wrapped around the WE; this configuration will establish oxygen-saturated or oxygen-depleted microenvironments during self-diagnosis phases. Proceeding from inside to outside, the next concentric circle can be used as the RE. The outermost electrode in Fig. 2 is the counter electrode (CE) of this three-electrode cell. It is placed at a distance from the WE to minimize electrochemical interference of byproducts generated at the CE. The counter GE, not shown, is located even more remotely from the WE for this same reason.

B. Microfabrication

All of the prototype sensors were fabricated in the facilities of the Biomedical Microsensors Laboratory (BMMSL), North Carolina State University [17]. All electrodes were platinum as shown in Fig. 2(b). Conventional platinum lift-off processes are difficult to execute on Kapton substrates when organic solvent-based photoresist chemistries are required. This is because the long immersion in the solvents required for lift off tends to degrade the adhesion of the metal to the Kapton substrate. On the other hand, wet chemical etching of platinum in heated aqua regia, while common on glassy substrates, was unsuccessful on Kapton substrates for undetermined reasons. Instead, the substrates were first metallized with chromium and gold, but these layers were left unpatterned until after the deposition and lift off of the platinum electrodes. This sequence has the advantage that the chromium and gold layer protects the Kapton substrate from contact with the solvents during titanium and platinum lift off.

Flexible polyimide substrates (Kapton, Du Pont, type VN, 75 μm in thickness), were cleaned in successive rinses of acetone, methanol, and deionized water, and then dehydrated at 120 $^{\circ}\text{C}$. A thin film of chromium as an adhesion layer, followed by a 0.2- μm film of gold, was deposited on the substrate by dc magnetron sputtering. Positive photoresist (Shipley 1813) was spin coated, selectively exposed through the photomasks with broad band UV light, and developed to pattern the electrode features. After deposition by dc magnetron sputtering of a thin titanium film and a 0.08- μm platinum film, the whole substrate was agitated in acetone to lift off the photoresist layer along with unwanted titanium and platinum. Positive photoresist (Shipley 1813) was spin coated again to protect the platinum layer during wet etching of the uncovered gold and chromium layers. After removal of the photoresist with solvents (Shipley 1165), the substrate was cleaned with organic solvents and dehydrated in preparation for the application of the polyimide dielectric layer. Photosensitive polyimide (HD Microsystems, Pyralin PI-2723) was spin coated to a nominal thickness of 2.0 μm and exposed in the same manner as the photoresist. Subsequent development and thermal curing of the polyimide defined the platinum electrodes.

The use of a polyimide (Kapton) substrate, which can be implemented as a flexible planar microsensor array, provides unique advantages for this specific application especially in terms of immunity to motion artifacts. Metal patterning to 10- μm linewidth was achieved. Smaller line widths are possible, but are more difficult due to thermal expansion of the Kapton substrate during the microfabrication process and surface roughness of the substrate. The electrochemical properties of each sensor from same wafer were showed some nonuniformity. In the future, we envision an optimized microfabrication process that includes more precise photolithography with higher resolution and the supporting the flexible substrate during processing with a rigid wafer to minimize thermal instability and substrate roughness.

C. Measurements

The fabricated Kapton-based oxygen microsensor was connected to the test instruments via a zero-insertion force (ZIF) connector and cable as shown in Fig. 3. A commercial miniature RE (Harvard Apparatus, AH69-0024) was used in this study in place of the on-chip RE to avoid possible instability of thin film Ag/AgCl electrode caused by electrochemical crosstalk with hydrogen peroxide which is a byproduct of the reaction [18]. The sensor was placed in a measuring vessel and the solution was saturated with different oxygen/nitrogen gas ratios at room temperature. Oxygen tension in the bulk solution was monitored with a commercial oxygen meter (Instech, SYS203). All measurements were done in a stationary solution to prevent any solution convectional effects.

A custom set of electrochemical instrumentation has been employed. A potentiostat (Gamry Instruments, FAS1) and a galvanostat (Gamry Instruments, 750) were used to bias the three-electrode oxygen microsensor and to operate the GEs, respectively. These two modules were plugged into one control PC and operated in a floating-ground mode to prevent electrical interference between the two modules. The cathodic potential for

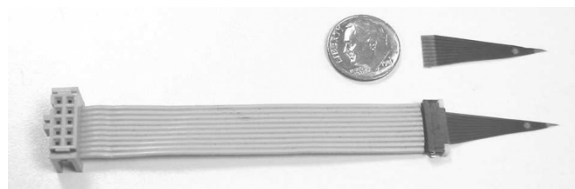


Fig. 3. Photograph of a probe assembly. An oxygen microsensor fabricated on flexible Kapton substrate (upper right part) is connected to a ribbon cable via a ZIF connector (lower part).

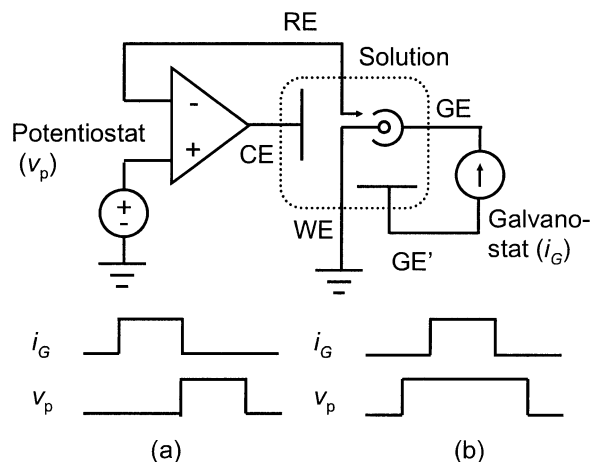


Fig. 4. Measurement scheme. A potentiostat and a galvanostat are employed for biasing the three-electrode oxygen microsensor and for generating microenvironments, respectively. (a) Sequential generating mode for transient response. (b) Simultaneous generating mode for quasi-steady-state response.

oxygen reduction (-0.7 V versus Ag/AgCl) was chosen from the plateau region in a traditional voltammogram. To control the microenvironment near the WE of the oxygen microsensor, constant currents were forced between the pair of generating and counter GEs. Fig. 4 shows a schematic of the measurement system.

A script was written to perform two different procedures for the establishment of microenvironments. First, the operation of the system was divided into a generation phase and followed by a measurement phase [Fig. 4(a)]. After a predefined gas-generating phase, the oxygen sensor was triggered by the potentiostat, which provides a potential step to the WE for oxygen reduction and then makes chronoamperometric measurements of the sensor's response. Any change in the microenvironment during the generating phase will affect transient response of the sensor. This two-phase process helps eliminate any possible electrostatic coupling between the three-electrode oxygen microsensor and the GE source. The second calibrating procedure involved a simultaneous gas-generating phase during sensor operation [Fig. 4(b)]. By this procedure, monitoring of any changes in the microenvironment during the preceding generating phase is possible by comparing real-time measurements with the sensor's baseline response, which reflects the background oxygen content. After each measurement, the solution was equilibrated to a defined baseline value by bubbling with a fixed ratio of oxygen and nitrogen gases and magnetically stirring.

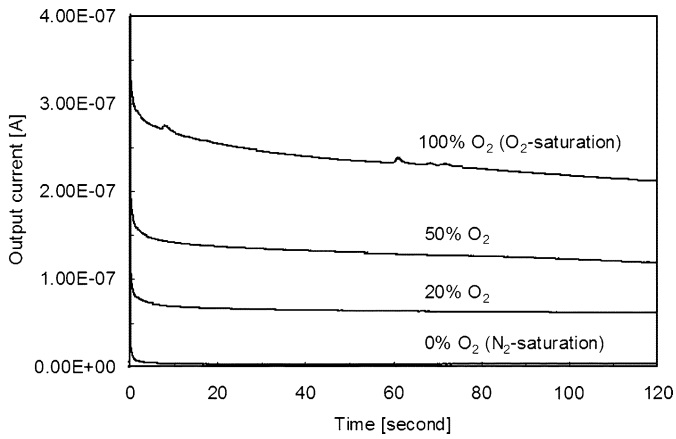


Fig. 5. Time responses (chronoamperometry) of the oxygen reduction current at a Pt WE responding to potential step (-0.7 V versus Ag/AgCl) in phosphate buffer solution (pH 7.4, 10 mM) with various oxygen contents.

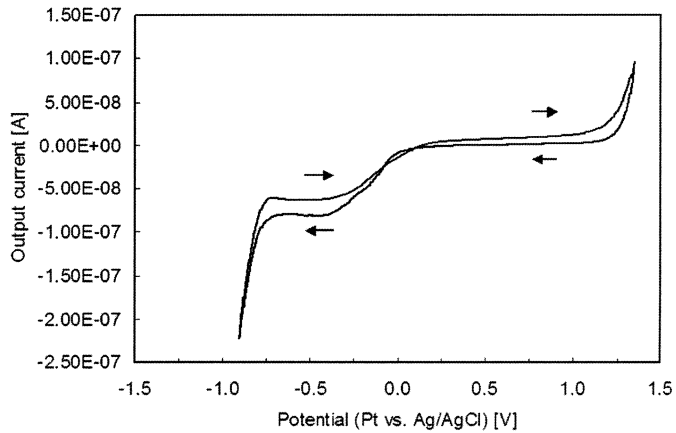
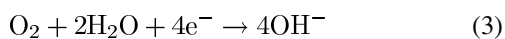


Fig. 6. Voltammogram of a Pt GE in air-saturated phosphate buffer solution (pH 7.4, 10 mM; scan rate: 50 mV/s).

IV. RESULTS AND DISCUSSION

A. Characterization of the WE and GE

Every new device was prepolarized for about 30 min at the cathodic potential for oxygen reduction (-0.7 V versus Ag/AgCl) before the actual measurements to obtain stabilized values. Fig. 5 shows typical chronoamperometric responses of the oxygen microsensor with a platinum WE in various bulk oxygen contents. Typical chronoamperometric responses are first observed at the onset of potential pulses to the WE. Afterward, the current reaches a steady-state value, which is called an oxygen limiting current. According to the limiting current theory, the relationship between limiting current magnitude and oxygen content is linear over the entire concentration range. The pH change during the oxygen reduction at the WE is considered to attribute to the nonlinearity of current magnitude versus oxygen content in Fig. 5. It is known that the stoichiometric coefficient of oxygen reduction, between 2.0 and 4.0, depends on bulk solution pH [19]. Oxygen reduction occurs predominantly in a single 4-electron step at low bulk solution pH



and an increase in bulk pH increases the proportion of two-electron step



As the oxygen concentration increases, the decrease in pH change at the surface of the WE (i.e., the accumulation of OH^- ions) becomes more significant to reduce the stoichiometric coefficient. Other factors that influence this coefficient, such as electrode material, reduction potential, surface aging, and pretreatment, remained the same in this study.

Fig. 6 shows a cyclic voltammogram of a platinum GE in an air-saturated phosphate buffer solution (10 mM, pH 7.4). Oxygen and hydrogen peaks can be seen at the right and left edges of the water electrolysis window, respectively. The minimum generating current was chosen to be 49 nA (0.5 mA/cm^2) for oxygen generation and -147 nA (-1.5 mA/cm^2) for oxygen depletion, respectively, to ensure high current efficiency for water electrolysis during the establishment of the microenvironments. Selecting a GE material with a narrower water electrolysis window will have benefits for this application by maximizing the current efficiency for electrolyzing water and minimizing the power consumption.

B. Transient Response Preceded by a Separate Generating Phase

Constant generating currents were driven through the generating (anode) and counter GEs (cathode) for up to 90 s to establish a stable microenvironment around the WE. Transient chronoamperometric responses in an air-saturated solution were recorded immediately following the generating phase as described in Fig. 4(a). As the duration of generating current pulses increases, the magnitudes of initial transient response increase as shown in Fig. 7(a). This means that a steady-state oxygen-rich environment has been established in the vicinity of the sensor as expected since a larger number of oxygen molecules were generated by the longer current durations. Convergence of all curves to bulk oxygen value (response to the air-saturated solution) means that the oxygen-rich environment is being equilibrated with the surrounding medium. With a generating current density of 5 mA/cm^2 the effect of generating current durations of longer than 30 s was about the same, suggesting that the degree of oxygen accumulation around the sensor in the generating phase reaches steady-state after about 30 s. Shortly after the completion of these measurements in the air-saturated environment, the solution was saturated with 100% oxygen to compare the sensor response. Note that the initial peaks after the generation phase in the air-saturated solution approach that obtained in the oxygen-saturated solution. A similar procedure was then applied to observe the transient response of the sensor after an oxygen-depleting phase provided by reversing the current direction through the GE. Fig. 7(b) shows typical responses of another sensor from the same wafer. The response after the depleting phase shows a reduced initial height followed by a recovery to the bulk response.

The main factors governing this microenvironment are the diffusion coefficient and mobility of the generated molecules (dissolved gases, hydrogen, and hydroxyl ions) in the sample

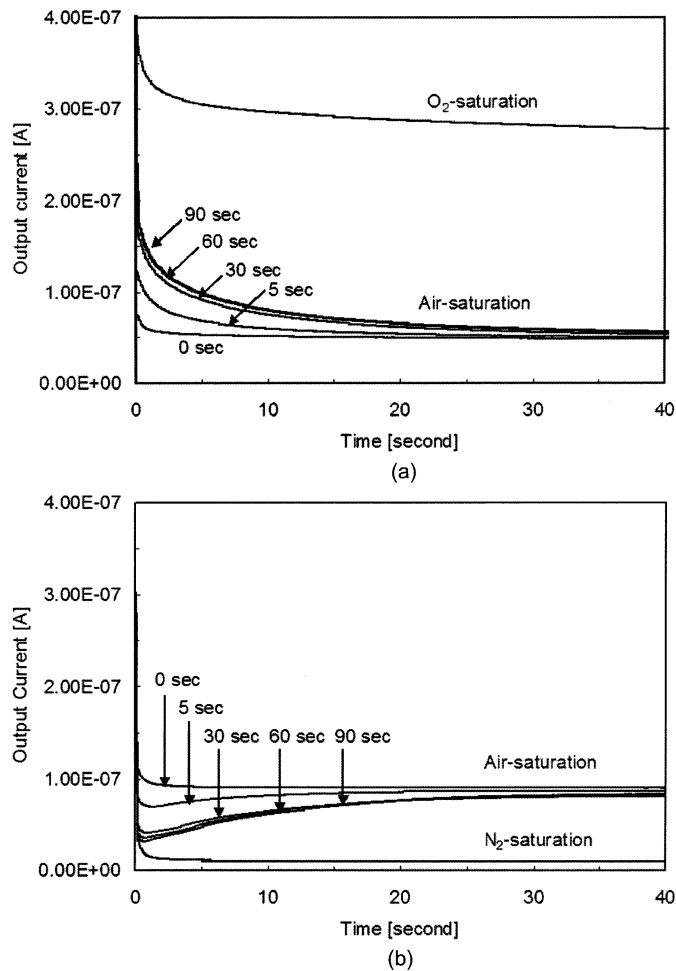


Fig. 7. Typical transient responses after an initial generating phase in air-saturated phosphate buffer solution (pH 7.4, 10 mM). (a) Effect of oxygen-generating phase with current pulses (5 mA/cm²) on the GE with various durations, with a sensor response to oxygen-saturated solution for comparison. (b) Effect of oxygen-depleting phase with current pulses (same pulse in the opposite polarity) on the GE with various durations, with a sensor response to nitrogen-saturated solution for comparison.

solution. These electrochemical parameters will be affected by the solution composition. Also the electrode kinetics (oxygen reduction at the WE, redox processes for oxygen/hydrogen generation, and hydrogen/hydroxyl ion production at the GE) may be affected by electrochemical interference of species in the sample solution. Sensor geometry, especially the spacing between working and GEs, will be the predominant parameter to determine the optimum conditions to control the microenvironment, which is a critical element in the performance of the *in-situ* self-diagnosis sensor. A small electrode area and close spacing between the electrodes is required to reduce the overall sensor size and to minimize oxygen consumption by the sensor itself. The sensor's geometric structure should be optimized to minimize the duration and magnitude of the generating signal.

C. Quasi-Steady-State Response During a Simultaneous Generating Phase

The generating phase was performed during the normal operation of the sensor for the mode of operation described

in Fig. 4(b). Once the limiting current condition at a given bulk oxygen content had been achieved after application of the oxygen reduction potential to the sensor, the generating current were applied to the GE for 90 s. The limiting current level (the baseline during the response) reflects the bulk oxygen content around the sensor. Various time responses during the generating phase are shown in Fig. 8(a). Simultaneous operation of the potentiostatic instrument (for biasing the oxygen microsensor) and the galvanostatic instrument (for driving the generating current) produced a quasi-steady-state response during the generating phase. For comparison the response to oxygen-saturation was recorded shortly after the completion of these measurements in the air-saturated case in the same solution. It can be seen that the responses during each generating phase approaches the limiting current levels of the oxygen-saturated solution and then gradually returns to the original level of bulk oxygen content. As the generating current density increases the corresponding response increases, which agrees with the result shown in Fig. 7(a). With the current density higher than 16 mA/cm², tarnish on the GE surface and damage to the polyimide encapsulation were observed occasionally in some of the devices.

At a given temperature, the limiting current magnitude in the oxygen-saturated solution (100% oxygen saturation) is limited to 4.76 times of that in the air-saturated solution (21% oxygen saturation) at 1 atm. During the generating phase with higher generating current densities, however, responses exceeding this limit were observed. The most plausible explanation for this is the supersaturation of the electrochemically generated oxygen in the microenvironment covering the WE [20]. The concentration of the electrochemically generated oxygen near the oxygen-evolving anode surface can exceed the standard oxygen solubility in water at 1 atm without the formation of gas bubbles. The pH change in the microenvironments due to water electrolysis is also expected to have contributed to this exaggerated response. The generation of dissolved oxygen and hydrogen is accompanied by a pH shift at the electrode surface, as shown in (1) and (2), which means the microenvironment will undergo pH changes during the generating phases. Subsequently, the oxygen catalytic activity of the platinum WE should be enhanced by the lower pH induced in the microenvironment according to (3) during this phase.

To observe the overall influence of pH and supersaturation, the generating phase was performed in an oxygen-saturated solution. The lower curve in Fig. 8(b) is a plot of the percent changes of response during the oxygen-generating phase with respect to the baseline at the oxygen-saturated solution. At the highest current density, the response was almost doubled from the baseline (response to the oxygen-saturated solution), suggesting that either the stoichiometric coefficient was increased or supersaturation was established, or both. To further investigate the influence of the pH changes during the oxygen-generating phase, measurements were performed in solutions with different pH buffering capacities. The response magnitudes in a 1-mM buffer solution were most pronounced, which implies that in stronger buffer solutions the pH changes were suppressed to minimize the perturbation of the stoichiometric coefficient of oxygen reduction. At the highest current

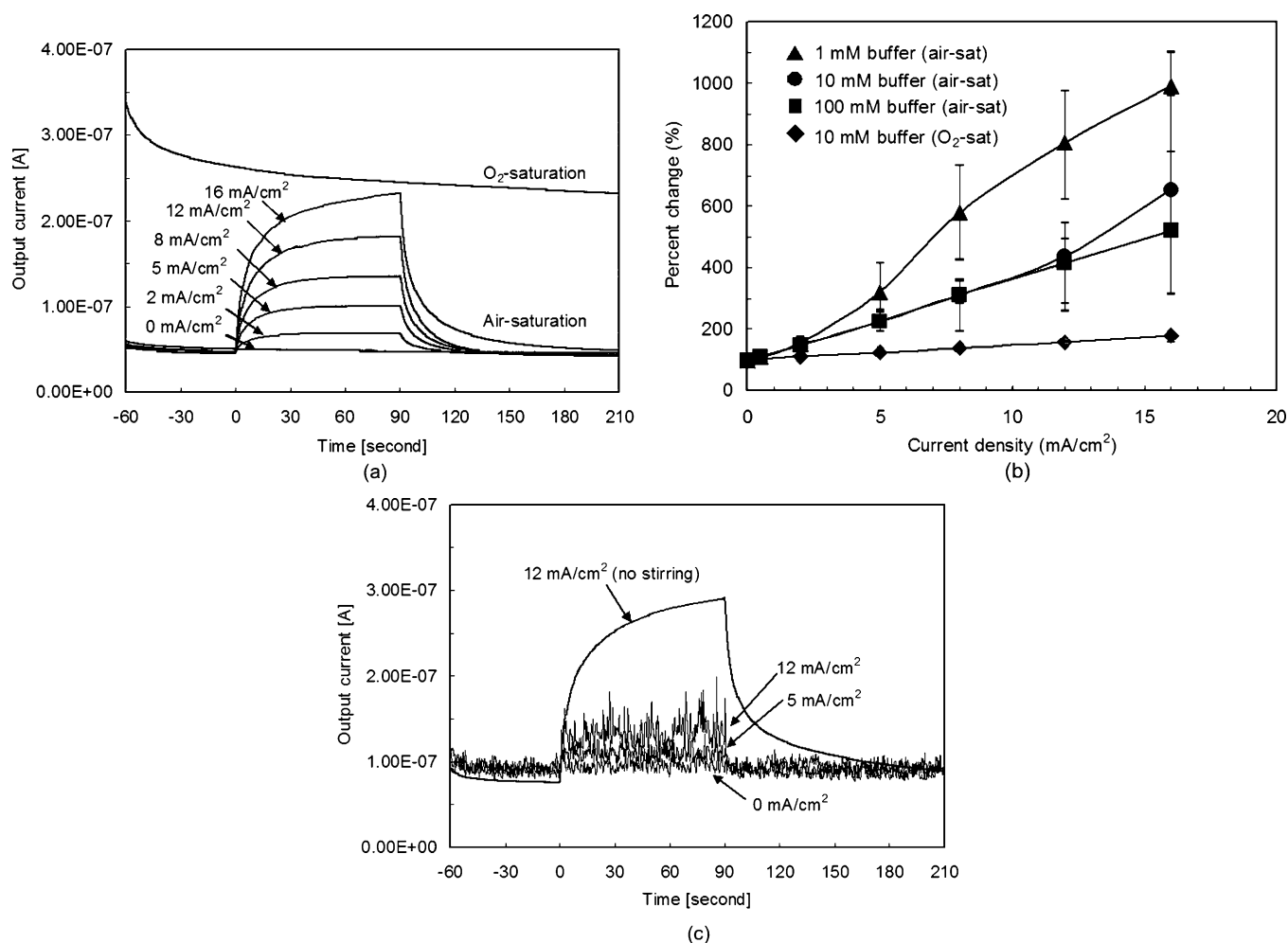
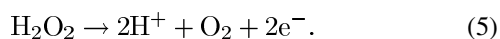


Fig. 8. Typical quasi-steady-state responses during the simultaneous oxygen-generating phase. (a) Effect of the oxygen-generating phase with various current densities in air-saturated phosphate buffer solution (pH 7.4, 10 mM), with a sensor response to oxygen-saturated solution for comparison. (b) Percent changes in the sensor responses (ratio of the steady-state value at $t = 90$ with respect to the baseline at $t = 0$) according to the generating current density in various pH buffering capacities, with those in an oxygen-saturated solution for comparison. (c) Effect of vigorous solution stirring in air-saturated phosphate buffer solution (pH 7.4, 10 mM), with a sensor response to a stationary solution for comparison.

density, the responses during the generating phase were similar with the oxygen-saturation value (theoretically 476%) in 10-mM and 100-mM buffer solution. This suggests that an *in-situ* high-point calibration (100% oxygen) can be accomplished by establishing an oxygen-saturated microenvironment with a refined device structure and generating signal.

Other factors may have contributed to the exaggerated responses; first, a considerable concentration-driven convection by the oxygen molecules diffusing from the GE could enhance the mass transport of oxygen in the stagnant solution, thereby increasing the limiting current value of the oxygen-saturated solution. A second factor may be “feedback” of electrochemically generated oxygen generated from hydrogen peroxide [18], a byproduct of oxygen reduction at the WE as in (4). Hydrogen peroxide is being oxidized to oxygen at the anodic GE and contributes to the oxygen-rich microenvironment



Third, the possibility of temperature elevation around the microsensor due to high current densities. The generation of gas

bubble has not been monitored during this study. Further analysis of these factors is necessary to adapt the proposed system for practical applications.

The effect of stirring on the microenvironment was also investigated. As expected, the magnitude of response diminished with energetic stirring of the solution as in Fig. 8(c). The response of the same sensor without solution stirring is given for comparison. Note the increased baseline produced by stirring. This result allows us to ascertain that the contribution of electrical interference to the response by the potentiostat operating the oxygen microsensor and the galvanostat operating the GE pair is negligible.

Fig. 9(a) shows the quasisteady state responses during the oxygen-depleting phase. Analogous to the generating phase, the sensor responses during depleting phases approach the limiting current levels at nitrogen-saturation, followed by a return to the original level of bulk oxygen content. As the current density increases the corresponding response decreases, which is consistent with Fig. 7(b). It should be noted from Fig. 9(b) that the responses with the current density higher than 5 mA/cm² remains around 30% of the bulk response without significant decrease beyond this level. This implies that the oxygen depletion

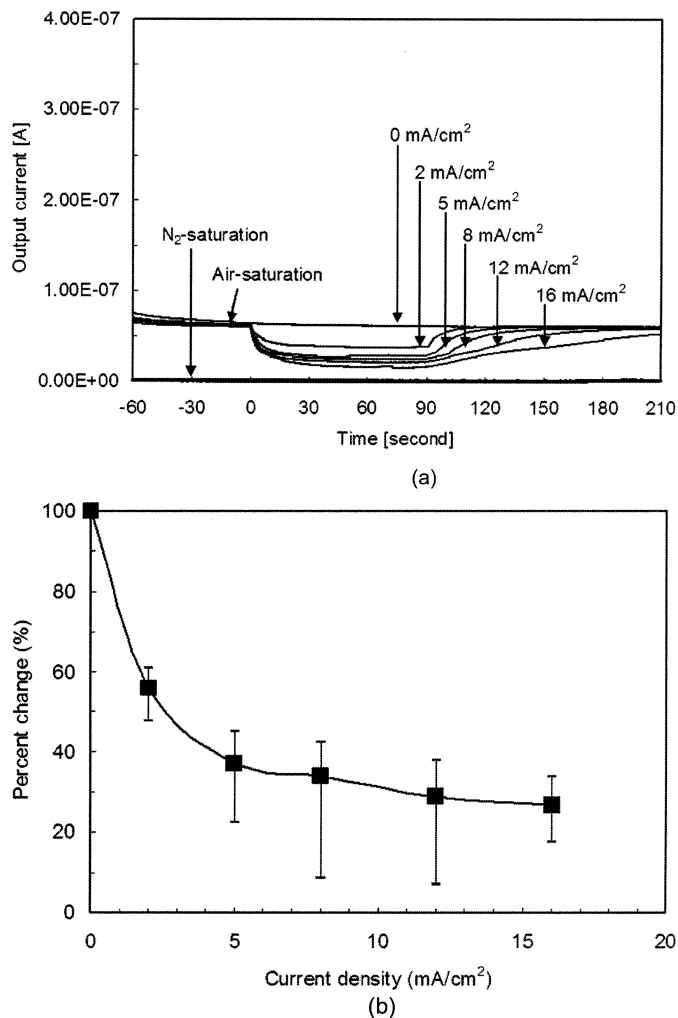


Fig. 9. Typical quasi-steady-state responses during the simultaneous oxygen-depleting phase in air-saturated phosphate buffer solution (pH 7.4, 10 mM). (a) Effect of the oxygen-depleting phase with various current densities, with a sensor response to nitrogen-saturated solution for comparison. (b) Percent changes in the sensor responses (ratio of the steady-state value at $t = 90$ with respect to the baseline at $t = 0$) according to the generating current density.

has not been completely accomplished with the given electrode geometry over the entire current density range. The higher pH in the microenvironment during the depleting phase is assumed to further decrease the sensor response due to the reduction of catalytic activity of the WE to reduce oxygen. Improvements in sensor structure are expected to achieve a low-point *in-situ* calibration during the sensor operation.

Incorporation of a Clark-type microsensor structure should minimize the pH effects and possible electrical interference caused by the galvanostat. By encapsulating a three-electrode oxygen sensor within a double-layer gas permeable membrane, consisting of an outer hydrophobic and an inner hydrophilic layer, the oxygen sensor itself can be fully isolated from the surrounding GE. However, microfabrication of a reliable and repeatable double-layered polymeric structure is challenging. In addition, lower oxygen permeability with the double-layer membrane will cause longer response time and will require a higher amplitude and longer duration of the generating signal.

V. CONCLUSION

The concept of an *in-situ* self-diagnostic technique for a dissolved oxygen microsensor is proposed in an effort to devise an intelligent microsensor system with an integrated electrochemical actuation electrode. The feasibility of the proposed concept is demonstrated in a physiological solution. The sensor responds properly during both the oxygen-generating and oxygen-depleting phases. The integrated electrochemical actuator is a useful tool for achieving built-in intelligence of the dissolved oxygen microsensor. The results suggest that the use of these microenvironments for *in-situ* self-diagnosis and *in-situ* self-calibration can be expected with carefully refined microstructures and generating signals. This intelligent capability of oxygen microsensors is needed to improve their reliability during their *in-situ* and, potentially, *in-vivo* operation.

REFERENCES

- [1] B. H. van der Schoot and P. Bergveld, "An ISFET-based microliter titrator: integration of a chemical sensor-actuator system," *Sens. Actuators*, vol. 8, pp. 11–22, 1985.
- [2] —, "Coulometric sensors: the application of a sensor-actuator system for long-term stability in chemical sensing," *Sens. Actuators*, vol. 13, pp. 251–262, 1988.
- [3] B. K. Sohn and C. S. Kim, "A new pH-ISFET based dissolved oxygen sensor by employing electrolysis of oxygen," *Sens. Actuators B*, vol. 34, pp. 435–440, 1996.
- [4] M. Lehmann, W. Baumann, M. Brischwein, H. J. Gahle, I. Freund, R. Ehret, S. Drechsler, H. Palzer, M. Kleintges, U. Sieben, and B. Wolf, "Simultaneous measurement of cellular respiration and acidification with a single CMOS ISFET," *Biosens. Bioelectron.*, vol. 16, no. 3, pp. 195–203, 2001.
- [5] J. Hendrikse, W. Olthuis, and P. Bergveld, "The ^EMOSFET as an oxygen sensor: constant current potentiometry," *Sens. Actuators B*, vol. 59, pp. 35–41, 1999.
- [6] D. T. V. Anh, W. Olthuis, and P. Bergveld, "Electroactive gate materials for a hydrogen peroxide sensitive ^EMOSFET," *IEEE Sensors J.*, vol. 2, pp. 26–33, Feb. 2002.
- [7] J. Wu and W. Sansen, "Electrochemical time of flight flow sensor," *Sens. Actuators B*, vol. 97–98, pp. 68–74, 2002.
- [8] A. Poghosian, J. W. Schultze, and M. J. Schoning, "Multi-parameter detection of (bio-)chemical and physical quantities using an identical transducer principle," *Sens. Actuators B*, vol. 91, no. 1–3, pp. 83–91, 2003.
- [9] B. H. van der Schoot, H. Voorthuyzen, and P. Bergveld, "pH-static enzyme sensor. Design of the pH control system," *Sens. Actuators B*, vol. 1, no. 1–6, pp. 546–549, 1990.
- [10] H. I. Seo, C. S. Kim, B. K. Sohn, T. Yeow, M. T. Son, and M. Haskard, "ISFET glucose sensor based on a new principle using the electrolysis of hydrogen peroxide," *Sens. Actuators B*, vol. 40, pp. 1–5, 1997.
- [11] F. Kreuzer, H. Kimmich, M. Brezina, and J. Heyrovsky, "Polarographic determination of oxygen in biological materials," in *Medical and Biological Applications of Electrochemical Devices*, J. Koryta, Ed. New York: Wiley, 1980, pp. 173–261.
- [12] I. Fatt, *The Polarographic Oxygen Sensor: Its Theory of Operation and Its Application in Biology, Medicine, and Technology*. Boca Raton, FL: CRC, 1976.
- [13] C. S. Kim, J. O. Fiering, C. W. Scarantino, and H. T. Nagle, "A novel *in situ* self-calibration method for an oxygen microsensor," in *World Congr. Medical Physics and Biomedical Engineering*, Chicago, IL, 2000.
- [14] M. Lambrechts and W. Sansen, *Biosensors: Microelectrochemical Devices*. Geneva, Switzerland: IOP, 1992, pp. 206–208.
- [15] G. Jobst, G. Urban, A. Jachimowicz, F. Kohl, O. Tilado, I. Letternbichler, and G. Nauer, "Thin-film Clark-type oxygen sensor based on novel polymer membrane systems for *in-vivo* and biosensor applications," *Biosens. Bioelectron.*, vol. 8, pp. 123–128, 1993.
- [16] P. Arquint, A. van den Berg, B. H. van der Schoot, N. F. de Rooij, H. Buhler, W. E. Morf, and L. F. J. Durselen, "Integrated blood-gas sensor for pO₂, pCO₂ and pH," *Sens. Actuators B*, vol. 13–14, pp. 340–344, 1993.

- [17] R. P. Buck, V. V. Cosofret, E. Lindner, S. Ufer, M. B. Madaras, T. A. Johnson, R. B. Ash, and M. R. Neuman, "Microfabrication technology of flexible membrane-based sensors for in-vivo applications," *Electroanal.*, vol. 7, pp. 846–851, 1995.
- [18] C. S. Cha, M. J. Shao, and C. C. Liu, "Problems associated with the miniaturization of a voltammetric oxygen sensor: chemical crosstalk among electrodes," *Sens. Actuators B*, vol. 2, pp. 239–242, 1990.
- [19] V. Linek, V. Vacek, J. Sinkule, and P. Benes, *Measurement of Oxygen by Membrane-Covered Probes*: Ellis Horwood, 1988, pp. 17–24.
- [20] S. Bohm, W. Olthius, and P. Bergveld, "An integrated micromachined electrochemical pump and dosing system," *J. Biomed. Microdevices*, vol. 1, no. 2, pp. 121–130, 1999.



Chang-Soo Kim (S'95–A'95–M'01) received the B.S., M.S., and Ph.D. degrees in electronic and electrical engineering from Kyungpook National University, South Korea, in 1989, 1991, and 1997, respectively.

During his graduate study, he worked on integrated circuit technologies and their applications to microsensors, especially for ISFETs. As a Research Associate at the Sensor Technology Research Center, South Korea, he was involved in various research projects and commercial development of

microelectrochemical sensors and systems for the monitoring of gases, electrolytes, and biomolecules. At the Biomedical MicroSensors Laboratory, North Carolina State University, Raleigh, and the Experimental Cardiology Group, University of North Carolina, Chapel Hill, he conducted postdoctoral research on intelligent biochemical sensors, implantable devices platforms, and cardiac biopotential recording with micromachined probes. He joined the University of Missouri-Rolla in 2002 as an Assistant Professor with a joint appointment at the Departments of Electrical and Computer Engineering and Biological Sciences. His current research interests include autonomous microsystem technology by functional and structural integration and novel applications of microsystem to plant research and space microgravity environment.

Dr. Kim is a member of ASEE and Sigma Xi.



Chae-Hyang Lee received the B.S. degree in physics from the Catholic University of Daegu, South Korea, in 1996 and the M.S. degree in sensor engineering from Kyungpook National University, South Korea, in 1998. She is currently pursuing the Ph.D. degree at Kyungpook National University.

During her M.S. study, her research focused on a novel potentiometric glucose microsensor with high sensitivity by using an electrochemical technique. She joined AUK, Ltd., South Korea, where she worked on the fabrication and characterization of

GaN light-emitting diode using MOCVD and photolithography processes. She is a Visiting Research student at the University of Missouri-Rolla.



Jason O. Fiering received the B.S. degree (with honors) in physics from Wesleyan University, Middletown, CT, and the M.S. degree in physics from Duke University, Durham, NC.

He has focused on microsystems and micro-fabrication for biomedical applications, first at the Biomedical Engineering Department, Duke University, Durham, NC, then at the Department of Electrical and Computer Engineering, North Carolina State University, Raleigh, and presently as a Senior Member of the Technical Staff, Draper

Laboratory, Cambridge, MA. His experience includes microdevice design and fabrication process development for applications including microfluidic systems, electromechanical drug delivery devices, ultrasound imaging transducer arrays, and electrochemical sensors for cardiology research. He was first introduced to microfabrication while a Research Associate at Bell Laboratories, Murray Hill, NJ. He was a Thomas J. Watson Fellow from 1990 to 1991, and he holds three patents with several others pending.



Stefan Ufer (S'95–A'00) received the Diploma in chemistry from the University of Muenster, Germany. He is currently pursuing the Ph.D. degree at the Chemistry Department, University of North Carolina, Chapel Hill.

He is the Operations Manager of the Biomedical MicroSensors Laboratory, Department of Biomedical Engineering, North Carolina State University, Raleigh. His research interests focus on microfabricated electrode arrays for biomedical applications.



Charles W. Scarantino received the B.S. degree from the Bloomsburg University of Pennsylvania, Bloomsburg, the Ph.D. degree in cell physiology, with a concentration in the identification of the hematopoietic stem cell, from St. John's University, Jamaica, NY, and the M.D. degree from the Bowman Gray School of Medicine, Wake Forest University, Winston-Salem, NC. He received his residency training in radiation oncology from the University of Rochester Strong Memorial Hospital, Rochester, NY.

He is a Staff Radiation Oncologist at the Rex Healthcare Cancer Center, Raleigh, NC. He is the former Vice Chair of the Cancer Control of the Radiation Therapy Oncology Group (RTOG) and is currently on its Executive Committee. Dr. Scarantino is published in clinical trials in radiation oncology, concerned with symptom management and combined modality therapy. He is the Co-Founder and Medical Director of Sidel Technologies, Inc., Morrisville, NC, a medical device company which has developed an implantable sensor platform technology to monitor *in-vivo* activities related to the therapy of malignant disease.

Dr. Scarantino is a Fellow of the American College of Radiation Oncology (ACRO) and a member of American Society of Therapeutic Radiation Oncology and the American College of Radiology.



H. Troy Nagle (S'66–M'70–SM'74–F'83) received the B.S.E.E. and M.S.E.E. degrees from the University of Alabama, Tuscaloosa, the Ph.D. degree in electrical engineering from Auburn University, Auburn, AL, and the M.D. degree from the University of Miami School of Medicine, Miami, FL.

He is a Professor and Founding Chair of the Joint University of North Carolina, Chapel Hill/North Carolina State Department of Biomedical Engineering and Professor of Electrical and Computer Engineering at North Carolina State University (NCSU),

Raleigh. He is the Director of BME's Biomedical MicroSensors Laboratory, NCSU, a 3 000 square-foot cleanroom facility with state-of-the-art sensor microfabrication capabilities. He is widely published in data acquisition and signal processing and is the coauthor of textbooks in digital logic design (with Victor P. Nelson, Bill D. Carroll, and J. David Irwin) and sampled-data-control systems (with Charles L. Phillips). Over the last several years, he has developed an electronic nose prototype and has experimented with its use in food processing, environmental monitoring, and medical diagnostics. Recently, he co-edited a handbook on machine olfaction (with Tim C. Pearce, Susan S. Schiffman, and Julian W. Gardner) published by Wiley VCH.

Dr. Nagle is a member of Phi Kappa Phi, Tau Beta Pi, Eta Kappa Nu, Sigma Xi, and Omicron Delta Kappa. He is a Fellow of AIMBE. He is a recipient of the IEEE Richard M. Emberson Award for outstanding service to the Institute in technical activities. He was the President of the IEEE Industrial Electronics Society (IES) from 1984 to 1985, Chairman of the IEEE Neural Networks Committee in 1988, and IEEE Vice President for Technical Activities from 1989 to 1990. He served as IEEE President in 1994, Chair of the IEEE Awards Board from 2000 to 2001, and Chair of the IEEE Medal of Honor Selection Committee from 2002 to 2003. He is currently a member of the IEEE Sensors Council and Editor-in-Chief of the IEEE SENSORS JOURNAL. He is a registered professional engineer.